Neuroscience 332 (2016) 170–180

PARKINSON SUBTYPE-SPECIFIC GRANGER-CAUSAL COUPLING AND COHERENCE FREQUENCY IN THE SUBTHALAMIC AREA

ESTHER FLORIN, [a,b]* **JOHANNES PFEIFER,** [c] **VEERLE VISSER-VANDEWALLE,** [d] **ALFONS SCHNITZLER** [b] **AND LARS TIMMERMANN** [a]*

[a] *Department of Neurology, University Hospital Cologne, Kerpener Strasse 62, 50937 Köln, Germany*

[b] *Institute of Clinical Neuroscience and Medical Psychology, Medical Faculty, Heinrich-Heine University Düsseldorf, Germany*

[c] *Department of Economics, University of Mannheim, Germany*

[d] *Department of Stereotaxy and Functional Neurosurgery, University Hospital of Cologne, Germany*

Abstract—Previous work on Parkinson's disease (PD) has indicated a predominantly afferent coupling between affected arm muscle activity and electrophysiological activity within the subthalamic nucleus (STN). So far, no information is available indicating which frequency components drive the afferent information flow in PD patients. Non-directional coupling e.g. by measuring coherence is primarily established in the beta band as well as at tremor frequency. Based on previous evidence it is likely that different subtypes of the disease are associated with different connectivity patterns. Therefore, we determined coherence and causality between local field potentials (LFPs) in the STN and surface electromyograms (EMGs) from the contralateral arm in 18 akinetic-rigid (AR) PD patients and 8 tremor-dominant (TD) PD patients. During the intraoperative recording, patients were asked to lift their forearm contralateral to the recording side. Significantly more afferent connections were detected for the TD patients for tremor-periods and non-tremor-periods combined as well as for only tremor periods. Within the STN 74% and 63% of the afferent connections are associated with coherence from 4–8 Hz and 8–12 Hz, respectively. However, when considering only tremor-periods significantly more afferent than efferent connections were associated with coherence from 12 to 20 Hz across all recording heights. No difference between efferent and afferent connections is seen in the frequency range from 4 to 12 Hz for all recording heights. For the AR patients, no significant difference in afferent and efferent connections within the STN was found for the different frequency bands. Still, for the AR patients dorsal of the STN significantly more afferent than efferent connections were associated with coherence in the frequency range from 12 to 16 Hz. These results provide further evidence for the differential pathological oscillations and pathways present in AR and TD Parkinson patients. **© 2016 IBRO. Published by Elsevier Ltd. All rights reserved.**

Key words: deep brain stimulation, connectivity, directionality, coherence, human, subthalamic nucleus.

INTRODUCTION

Parkinson's disease (PD) is characterized by pathological oscillations within the subthalamic nucleus (STN) and motor cortex (Volkmann et al., 1996; Timmermann et al., 2003; Kühn et al., 2006; Brown, 2007). Much of the previous work has either focused on analyzing the frequency components of these pathological oscillations (Kühn et al., 2006; Reck et al., 2009b; Hirschmann et al., 2013) or the directionality of such a pathological coupling (Florin et al., 2010b). In particular, with coherence-based analysis different pathological frequency ranges have been found for the different Parkinson subtypes, akinetic-rigid (AR) and tremor-dominant (TD). In the case of AR patients, excessive beta oscillations (12–30 Hz) are a pathological hallmark (Brown et al., 2001; Silberstein et al., 2003; Kühn et al., 2004; Chen et al., 2007). For TD patients the oscillations are increased in the tremor (4–8 Hz) and double-tremor frequency range (Timmermann et al., 2003; Reck et al., 2009b, 2010). These two different findings indicate that subtype-specific pathophysiological changes are found in PD.

Furthermore, our own previous work has indicated that the coupling between affected arm muscle activity and electrophysiological activity within the STN is predominantly afferent during the main motor symptom of the particular Parkinson subtype (Florin et al., 2010b, 2012). Additionally, an optogenetic study in Parkinsonian rodents has shown that stimulation of the afferent axons projecting to the STN alleviates the motor symptoms (Gradinaru et al., 2009). However, so far no information on the frequency specificity of the afferent connections has been provided. This stems from a limitation of Granger based causality measures, which are often used to determine the directionality of the coupling. Due to a low determined model order of the autoregressive

*Corresponding authors. Address: Institute of Clinical Neuroscience and Medical Psychology, Medical Faculty, Heinrich-Heine University Düsseldorf, Germany (E. Florin). Fax: +49-221-87512 (L. Timmermann).

E-mail addresses: Esther.Florin@hhu.de (E. Florin), Lars.Timmermann@uk-koeln.de (L. Timmermann).

Abbreviations: AR, akinetic-rigid; DBS, deep brain stimulation; EDC, M. extensor digitorum communis; EMG, electromyogram; FDI, first dorsal interosseous muscle; FDL, M. flexor digitorum superficialis; fMRI, functional magnetic resonance imaging; LFPs, local field potentials; LOOM, leave one out method; MVAR, multivariate autoregression; PD, Parkinson's disease; sPDC, squared partial directed coherence; STN, subthalamic nucleus; TD, tremor-dominant.

http://dx.doi.org/10.1016/j.neuroscience.2016.06.052
0306-4522/© 2016 IBRO. Published by Elsevier Ltd. All rights reserved.

model – on which the estimation of Granger causality is often based – the frequency resolution in many real data applications is not high enough to distinguish the physiological frequency ranges (Schlögl and Supp, 2006). The aim of the present study is to provide insights into the frequency specificity of directional information with respect to different subtypes of PD by jointly studying the relationship between coherence and directionality.

We analyzed recordings from Parkinson patients who underwent an implantation of deep brain stimulation (DBS) electrodes. During this implantation of DBS electrodes we simultaneously recorded local field potentials (LFPs) from above and within the STN and electromyographic (EMG) activity from affected contralateral arm muscles. We combined coherence and causality analysis to gain additional information on the connections between LFPs and affected arm muscles. For the causality analysis we used the squared partial directed coherence (sPDC) (Astolfi et al., 2006). While causality and coherence in principle analyze different temporal components (temporal shift vs. contemporaneous), their joint behavior is nonetheless informative about the connection between arm-muscle activity and LFPs in the STN.

Based on the subtype-specific frequency changes in PD (Brown et al., 2001; Silberstein et al., 2003; Kühn et al., 2004; Chen et al., 2007), the two specific hypotheses tested are (1) that the detected causalities in the case of AR patients co-occur with coherence in the beta band and (2) that in the case of TD patients the co-occurrence is mainly in the tremor-frequency range. The frequency specificity within these hypotheses is based on the previous literature on oscillatory activity in PD.

EXPERIMENTAL PROCEDURES

Patients

For this study we included all Parkinson patients from 2005 to 2008 who (i) underwent DBS implantation in the STN at our center and (ii) had recordings of LFPs during an isometric hold condition. The clinical preoperative decision for the implantation of DBS electrodes was made in accordance to the guidelines in Lang et al. (2006) and Hilker et al. (2009). After excluding patients with incomplete clinical information (no pre- and postoperative UPDRS), 18 AR PD patients with 24 recorded hemispheres and 8 TD PD patients with 9 recorded hemispheres were included for this study. We have analyzed data from these patients in our previous studies (Reck et al., 2009a, 2009b, 2010; Florin et al., 2010b, 2012, 2013a, 2013b), but focused on different aspects in the recordings than in the current study. The Parkinson patients were classified as AR, TD and mixed type based on their UPDRS score according to Spiegel et al. (2007). The mixed type and TD patients were grouped together, because all these patients had a higher tremor than akinesia score. A summary of preoperative data is given in Table 1.

All patients gave written informed consent to the implantation of electrodes and the micro- and macroelectrode recordings. The study was approved by the local ethics committee (study no. 2459 and 08-158) and conducted in accordance with the Declaration of Helsinki.

Implantation and intra-operative recordings

The implantation and intra-operative recording procedure has been described in detail in Florin et al. (2012). Dopaminergic medication was withdrawn for at least 12 h before operation to minimize its influence during the operation. Clinically this allows for testing the stimulation parameters during the operation without confounds from the medication. During implantation, LFPs were recorded with up to five combined micro- and macroelectrodes using the INOMED ISIS MER-system (INOMED corp., Teningen, Germany). Less than five micro–macroelectrodes were used in patients where the individual anatomy and blood vessels did not allow for all five electrodes. Simultaneously, surface EMGs were recorded of the M. extensor digitorum communis (EDC), M. flexor digitorum superficialis (FDL), and the first dorsal interosseous muscle (FDI) with the INMOED ISIS MER-system. Patients were asked to lift their forearm contralateral to the recording side for at least 30 s. For the tremor patients we included periods both with and without postural tremor. In a subanalysis we further separated these recordings into periods with postural tremor and without tremor. The sampling rate of the EMG and LFP signals was 2500 Hz. During the recording a high-pass filter of 0.5 Hz and a low-pass filter of 1 kHz was used. The LFPs were recorded from at most 9 mm above the target point in the STN. The recording was continued in steps of 1 mm downwards until up to 1 mm below the target point within the STN. An example recording is displayed in Fig. 1. Based on the discharge pattern from the microelectrode recording the location was either classified as within the STN or above the STN. For details on this please refer to Reck et al. (2010).

Statistical causality analysis with squared partial directed coherence (sPDC)

After the implantation, macroelectrode and EMG recordings from each patient were visually reviewed to detect artifacts. In the case of an artifact the respective sequences were excluded from further analysis. Only consecutive sequences of at least 10 s were used. The EMGs were 2 Hz high-pass filtered to remove drifts due to movements. Both LFPs and EMGs were 50 Hz notch filtered to remove potential electric artifacts. These filter settings are in accordance with our previous simulation study, where we demonstrated their compatibility with statistical causality analysis (Florin et al., 2010a), and are the same as in Florin et al. (2012). In addition the recordings were z-scored to normalize the amplitudes between EMG and LFP. Matlab (version 8.2., The MathWorks, Inc., Natick, MA, USA) and the Biosig-toolbox (version 1.97) (http://biosig.sourceforge.net) were used for the analysis.

For the statistical causality analysis we used a multivariate extension of Granger causality (Granger, 1969) in the spectral domain: the sPDC (Astolfi et al.,

Table 1. A total of 26 PD patients were included. The number of trajectories indicates the number of recording electrodes for the respective implantation side. Abbreviations: m = male, f = female, L = left, R = right; UPDRS – motor score of the Unified Parkinson's disease rating scale; ON – with medication; OFF – without medication; AR – akinetic-rigid subtype; TD – tremor-dominant subtype

Patient no.	Gender	Age	Disease duration	UPDRS ON	UPDRS OFF	Subtype	Recording side	# Trajectories
1	f	70	13	17	32	AR	STN (L)	4
2	m	58	9	43	54	AR	STN (L)	5
3	f	71	10	14	40	AR	STN (L + R)	5/5
4	f	58	14	14	41.5	AR	STN (L)	5
5	f	44	6	9	31	AR	STN (L)	4
6	m	70	17	25	43	AR	STN (L + R)	5/5
7	f	46	5	7	27	AR	STN (L)	5
8	f	66	18	29	58	AR	STN (L)	5
9	f	64	20	21	64	AR	STN (L + R)	5/3
10	m	70	13	14	32	AR	STN (L + R)	4/5
11	m	61	10	23	35	AR	STN (L + R)	5/3
12	m	57	3	13	33	AR	STN (L)	5
13	m	69	18	20	32	AR	STN (L)	4
14	m	62	12	24	60	AR	STN (L)	3
15	m	71	10	27	56	AR	STN (L + R)	4/4
16	m	74	17	18	38	AR	STN (L)	5
17	m	63	9	25	62	AR	STN (L)	3
18	f	66	14	27	37	AR	STN (L)	4
19	m	53	4	25	32	TD	STN (R)	4
20	m	71	8	22	59	TD	STN (L)	4
21	m	70	11	15	42	TD	STN (R)	4
22	m	76	8	40	46	TD	STN (R)	5
23	m	72	12	17	35	TD	STN (L)	3
24	m	73	7	38	50	TD	STN (L + R)	5/5
25	m	60	12	3	11	TD	STN (L)	4
26	f	65	10	35	44	TD	STN (L)	4

2006). The sPDC was the most robust measure in simulations (Florin et al., 2011). The sPDC analysis follows the same lines as in our previous publications: For the multivariate autoregression (MVAR) the model order was determined by using the Bayesian information criterion (BIC) and the significance threshold for the individual statistical causalities was computed by the leave-one-out method (LOOM) (Efron, 1981; Schlögl and Supp, 2006). The significance threshold was set at 95%.

Coherence

Even though the sPDC is a frequency domain measure, based on the sampling rate and the model order between 8 and 50 for our data we cannot obtain a sufficient frequency resolution to distinguish typical physiological frequency bands (Schlögl and Supp, 2006): Only as many frequency components as the chosen model order can be modeled. With our sampling rate of 2500 Hz in the best case this leads to a frequency resolution of about 50 Hz. For a better frequency resolution a higher model order than the optimal one would be required. This, however, decreases the efficiency of the MVAR-estimation and increases the likelihood of false statistical causalities. Therefore, we additionally used coherence to gain further frequency information for the analyzed connections between EMG and LFP. Note that the sPDC, using the Wiener–Granger notion of causality, is based on an information set only containing past time points whereas a conventional coherence between two signals considers the instantaneous correlation. Therefore the presence of one of the relations does not imply the other.

Within this present analysis we do not consider connections where a bidirectional coupling was identified with the sPDC. For the frequency analysis we used the coherence $C_{XY}(f)$ at frequency f between the signals X and Y (Halliday et al., 1995):

$$C_{XY}(f) = \frac{|S_{XY}(f)|}{\sqrt{S_{XX}(f)S_{YY}(f)}} \quad (1)$$

$S_{XY}(f)$ is the cross-spectrum and $S_{XX}(f)$ and $S_{YY}(f)$ are the auto-spectra of the time series. We calculated the coherence based on periodograms with half-overlapping Hanning windows and averaged the periodograms. The significance threshold was determined according to Schelter et al. (2006) and Halliday et al. (1995):

$$Coh_{crit} = \sqrt{1 - \alpha^{2/(\nu-2)}} \quad (2)$$

We chose the significance level α at 0.01. The effective degrees of freedom ν were determined for half-overlapping windows in accordance to Welch (1967):

$$\nu = 2.8 \cdot N \cdot \frac{7}{6L} \quad (3)$$

N are the total data points and L is the chosen window length of each periodogram. In the present study the window length was 5120 data points, leading to a frequency resolution of about 0.5 Hz. We binned the coherence values in 4 Hz steps from 4 to 28 Hz. This frequency range was chosen to include the tremor frequencies (4–8 Hz) and the beta band (12–28 Hz).

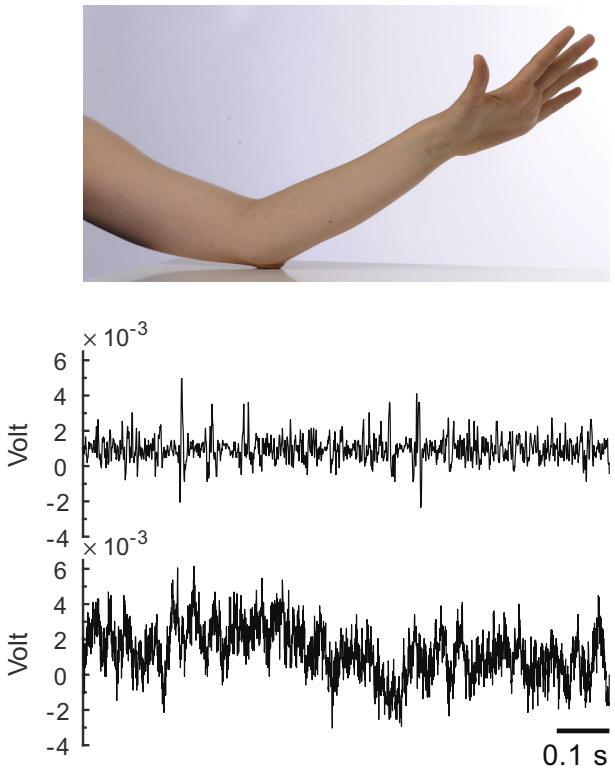

Fig. 1. Paradigm and raw data. The top panel shows how the patients were requested to hold the arm upwards during the recording. This part has been modified from Reck et al. (2009a) and Reck et al. (2010). The lower panels display local field potential (middle) and EMG (bottom) recordings from patient 4. The local field potential was obtained from above the STN.

Additionally, we calculated the corrected coherence spectra $C_{XY}^{corr}(f)$ for all significant causal connections,

$$C_{XY}^{corr}(f) = \tanh^{-1}(C_{XY}(f)) - \frac{1}{\nu - 2}, \quad (4)$$

where the correction accounts for the different effective degrees of freedom resulting from different data lengths (Bokil et al., 2007).

The corrected power P^{corr} was determined as follows (Bokil et al., 2007):

$$P_{XX}^{corr}(f) = \log(P_{XX}(f)) - \psi\left(\frac{\nu}{2}\right) + \log\left(\frac{\nu}{2}\right) \quad (5)$$

Ψ is the polygamma function.

Statistical comparisons were made with binominal tests and Bonferroni corrected. The statistical analysis was conducted in SPSS (IBM SPSS statistics, release 20.0.0) and Matlab. Regression analysis was conducted using Matlab's robustfit-command, which conducts an iteratively reweighted least squares regression with a bisquare weighting function.

RESULTS

In total, we included 18 AR PD patients and eight TD patients. The age, disease duration, and UPDRS did not significantly differ between the two groups at the 5% level (*t*-test). A summary of the patient characteristics is given in Table 1 (AR: Age: 63.3 ± 8.4 years; disease duration: 12.1 ± 4.8 years; UPDRS OFF: 43.1 ± 12.8; UPDRS ON: 21.9 ± 7.9; TD: Age: 67.5 ± 7.7 years; disease duration: 9.0 ± 2.8; UPDRS OFF: 39.9 ± 14.4; UPDRS ON: 27.4 ± 9.5).

Overall, for the AR patients 4.5% of all potential connections were unilaterally causally linked from LFP to EMG and 3.1% from EMG to LFP (binomial test: $z = 2.07$, $p = 0.02$). This difference for the AR patients was significant both in the STN and above the STN (Within the STN: 5.7% vs 3.4% binomial test; $z = 1.86$, $p = 0.03$; Above STN: 4.4% vs 2.5%; $z = 2.10$, $p = 0.02$, see also Table 2). For the TD patients 5.3% of the connections were unilateral from LFP to EMG and 11.5% in the opposite direction. Hence, significantly more afferent connections were detected for the TD patients (binomial test; $z = 3.80$, $p = 0.00007$). This difference for the TD patients was also significant within the STN and the recordings above the STN (Within the STN: 3.5% vs 13.6% binomial test; $z = 3.59$, $p = 0.0002$; Outside STN: 6.3% vs 11.2%; $z = 1.99$, $p = 0.02$). Even though the total percentage might seem low, one has to keep in mind that we tested all recording heights and locations used during the DBS implantation, while a connection between LFP and arm muscle activity is only physiologically feasible in some of the analyzed regions. To get a better overview of the spatial distribution of detected afferent and efferent connections we renormalized the origin of the recording heights for each patient to the entry height of the central electrode in the STN. This entry point into the STN was accessed from the microelectrode recording. When conducting this normalization four patients had to be excluded, because their central electrode did not enter the STN. We then calculated the percentage of efferent and afferent connections across patients based on the total possible connections at each re-normalized recording height. For the display in Fig. 2, we excluded renormalized heights where only one patient was recorded and then fitted a second order polynomial via a least squares regression. Interestingly, for the efferences of the AR and TD patients a significant negative quadratic term was found (AR: $b = -0.18$; $p = 0.002$; TD: $b = -0.27$; $p = 0.011$).

For the next analysis step we subdivided the detected causal connections into those within the STN and those above the STN. The occurrences of causal connections within the STN and above the STN are summarized in Table 2. We calculated the coherence between the signals involved in these detected causalities and determined the frequency bands of significant coherence values. Fig. 3 shows these results for the AR and the TD patients. For the AR patients only outside the STN significantly more afferent than efferent connections were associated with a coherence in the frequency range from 12 to 16 Hz (Fig. 3; binomial test; $z = 2.50$; $p = 0.037$; Bonferroni corrected). For the TD patients no significant differences between efferent and afferent connections were found within a particular frequency range of the coherence. Within the STN, we observed that 74% and 63% of the afferent connections

Table 2. Number of significant unidirectional Granger causalities across patients

	LFP- > EMG	EMG- > LFP	Total	% LFP- > EMG	% EMG- > LFP	Range LFP- > EMG	Range EMG- > LFP
AR	70	48	1539	4.5	3.1	[0; 15]	[0; 17]
TD	31	67	582	5.3	11.5	[0; 11]	[0; 16]
AR within STN	32	19	557	5.7	3.4	[0; 10]	[0; 7]
TD within STN	7	27	198	3.5	13.6	[0; 5]	[0; 12]
AR above STN	34	19	774	4.4	2.5	[0; 8]	[0; 5]
TD above STN	17	30	268	6.3	11.2	[0; 8]	[0; 12]

Notes: "Total" refers to the total number of potential causalities, while "Range" refers to minimum and maximum values. Note that within and above STN do not sum to the total due to the presence of recording heights below the STN.

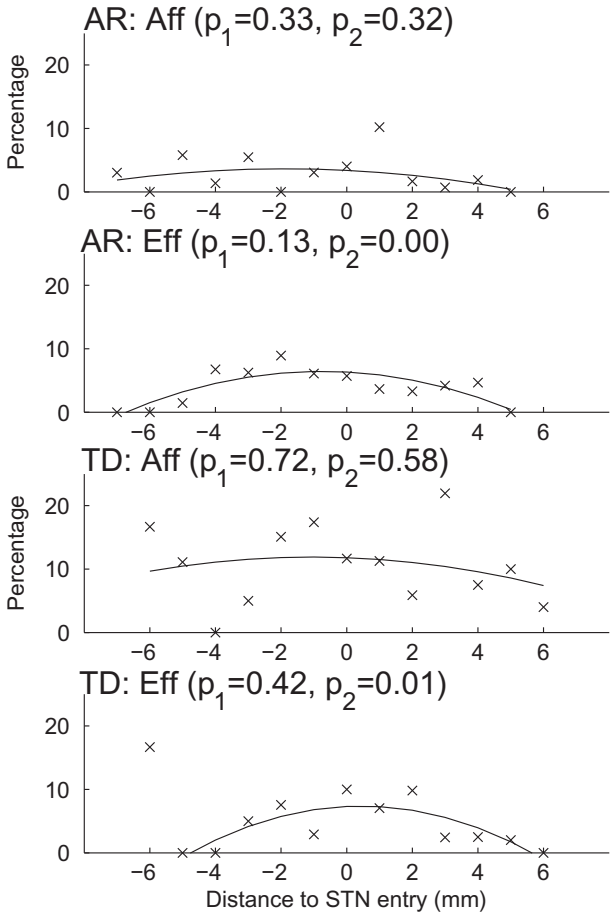

Fig. 2. Occurrence of afferences and efferences relative to the STN entry point. On the *x*-axis the distance of the recording height relative to the height of the entry point of the central electrode into the STN is displayed. Negative values indicate recordings above the STN. The *y*-axis displays the share of uni-directional connections relative to the possible connections. Only recording heights with at least two patients are included. The line displays predicted values from a quadratic polynomial fitted to the data via a robust least squares regression. In particular for the efferent connections an increase is found as the STN is approached. AR – akinetic-rigid; TD – tremor-dominant; STN – subthalamic nucleus; Aff – afference; Eff – efference; p_1 – *p*-value of linear term in polynomial fit; p_2 – *p*-value of quadratic term in polynomial fit.

co-occurred with a significant coherence in the tremor- and respectively the double tremor-frequency range.

Fig. 4 shows the averaged corrected coherence spectra for the two patient groups. These plots demonstrate a clear peak in the tremor-frequency band for the TD patients. In particular within the STN the coherence in the tremor-frequency range is higher for the afferent connections. The differences were, however, not significant after correcting for multiple comparison across all tested frequencies. In the case of the AR patients no clear peak is seen and no difference in the coherence between efferent and afferent connections is found.

We further investigated whether the co-occurrence of coherence and causality in the tremor-frequency band in the case of the TD patients is associated with the presence of tremor. For this purpose, we subdivided the data-set of the TD patients into periods with postural tremor and ones without. Not all patients had tremor and non-tremor periods during the hold condition at each recording height, leading to a smaller sample size in this analysis. The detected causalities for this smaller sample are listed in Table 3. Overall, there are a very low number of detected causalities for periods without tremor. Interestingly, when restricting our analysis to tremor-periods during hold, significantly more afferent than efferent connections co-occur with significant coherences in the beta frequency range (12–20 Hz) (Fig. 5; Binomial test for 12–16 Hz: $z = 2.42$; $p = 0.047$; 16–20 Hz: $z = 2.42$; $p = 0.047$; Bonferroni corrected). During periods without any tremor, significantly more efferent than afferent connections co-occur with a significant coherence from 20 to 24 Hz across all recording heights (binomial test for 20–24 Hz: $z = 2.63$; $p = 0.03$; Bonferroni corrected). When looking at the averaged power spectra and coherence spectra, a clear tremor-peak is seen for the tremor-periods, but not the periods without tremor (Fig. 6). For the afferent connections there is also a significant correlation between the EMG power at tremor-frequency and coherence at this frequency (rho = 0.43; $p = 0.00062$), which is not the case for the efferent connections (rho = −0.076; $p = 0.75$).

DISCUSSION

In the present study we aimed at identifying the Parkinson subtype-specific causal connections between subthalamic LFPs and affected arm muscle activity on the one hand and the frequency specificity of coherence between the signals involved in these connections on the other hand. For TD patients during tremor-periods and for the combined analysis of tremor- and non-tremor periods more afferent connections were found,

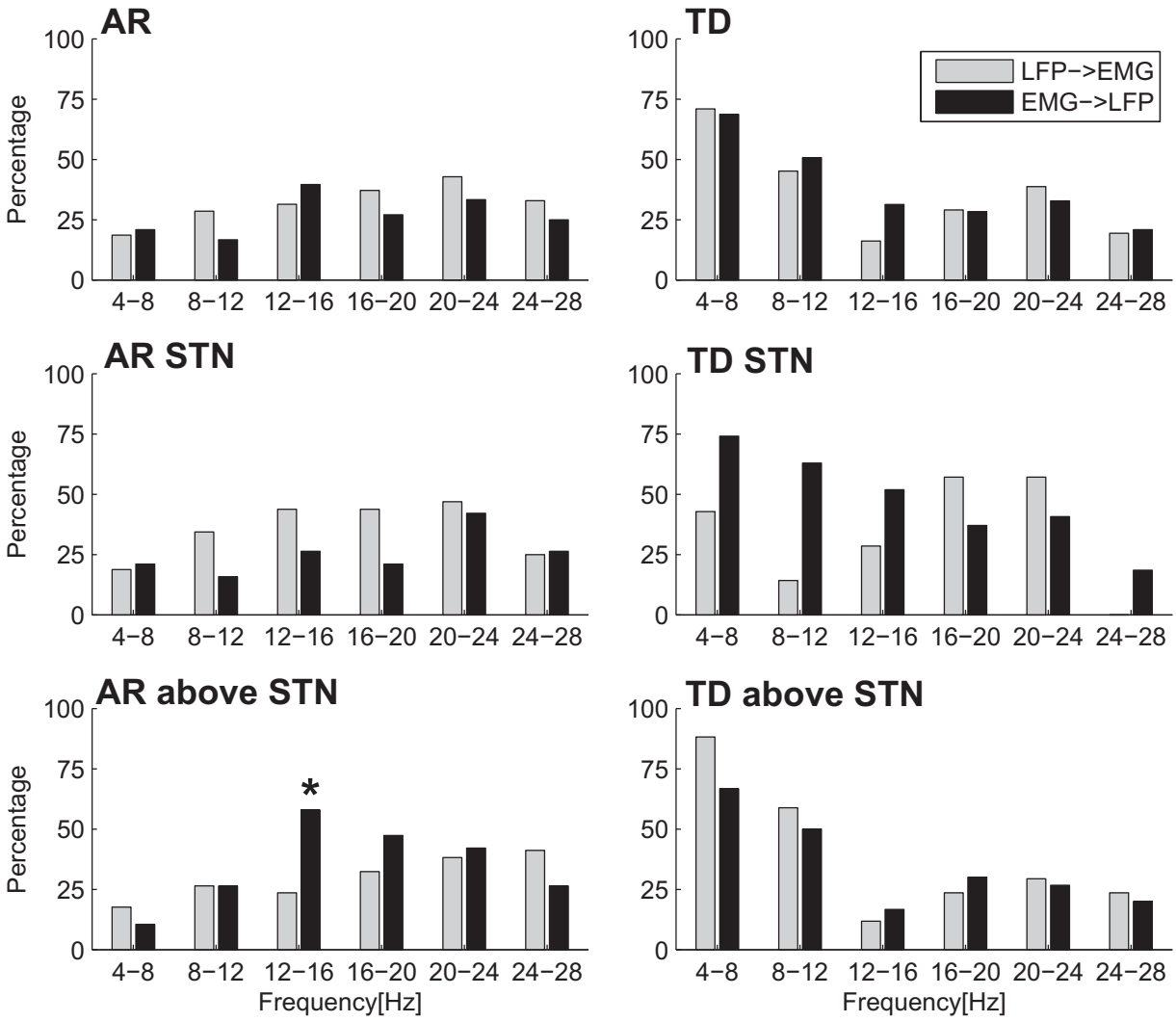

Fig. 3. Co-occurrence of significant causality and coherence for akinetic-rigid and tremor-dominant patients. The graphs display the percentage of connections with a significant coherence in the respective frequency band between EMG and LFP, conditional on the existence of significant unidirectional causal interactions. Above the STN for the AR patients significantly more afferent connections were associated with a coherence from 12 to 16 Hz. AR – akinetic-rigid; TD – tremor-dominant; STN – subthalamic nucleus; EMG – electromyogram; LFP – local field potential; * – $p \leqslant 0.05$ (see text for exact values).

whereas for the AR patients more efferent connections were detected. The significant coherence frequency for the afferent connections of the TD patients in a combined analysis of tremor and non-tremor periods was mainly in the double tremor-frequency within the STN, albeit no significant difference to the efferent connections was found. In contrast, for the AR patients a significantly higher number of afferent than efferent connections above the STN were associated with coherence in the low beta-frequency range (12–16 Hz).

Combination of coherence and Granger causality

To identify the frequency specificity, we combined coherence and Granger causality analysis. It is important to note that both measures use different temporal components of the connections and therefore are, mathematically speaking, not analyzing the same information flow. Still, both yield information on the connectivity between the analyzed regions. Kayser et al. (2009) previously compared coherence and Granger causality for functional magnetic resonance imaging (fMRI) data. In this case, coherence and Granger causality yielded similar results. This presumably stems from the fact that fMRI has a low temporal resolution that causes the distinction of sequentiality used in Granger causality and simultaneity used in coherence to become blurred. It is for that reason that the advantage of Granger causality to identify directionality information decreases when used in fMRI. In contrast, LFP recordings do not have the problem of a too low temporal resolution for Granger causality. Hence, the combination with coherence allowed us to obtain further frequency information on the connections that exhibit causal relations. This is generally not possible with the Granger-based causality analysis on electrophysiological data. The frequency limitation of Granger causality stems from the fact that only as many frequency components as the chosen model order can

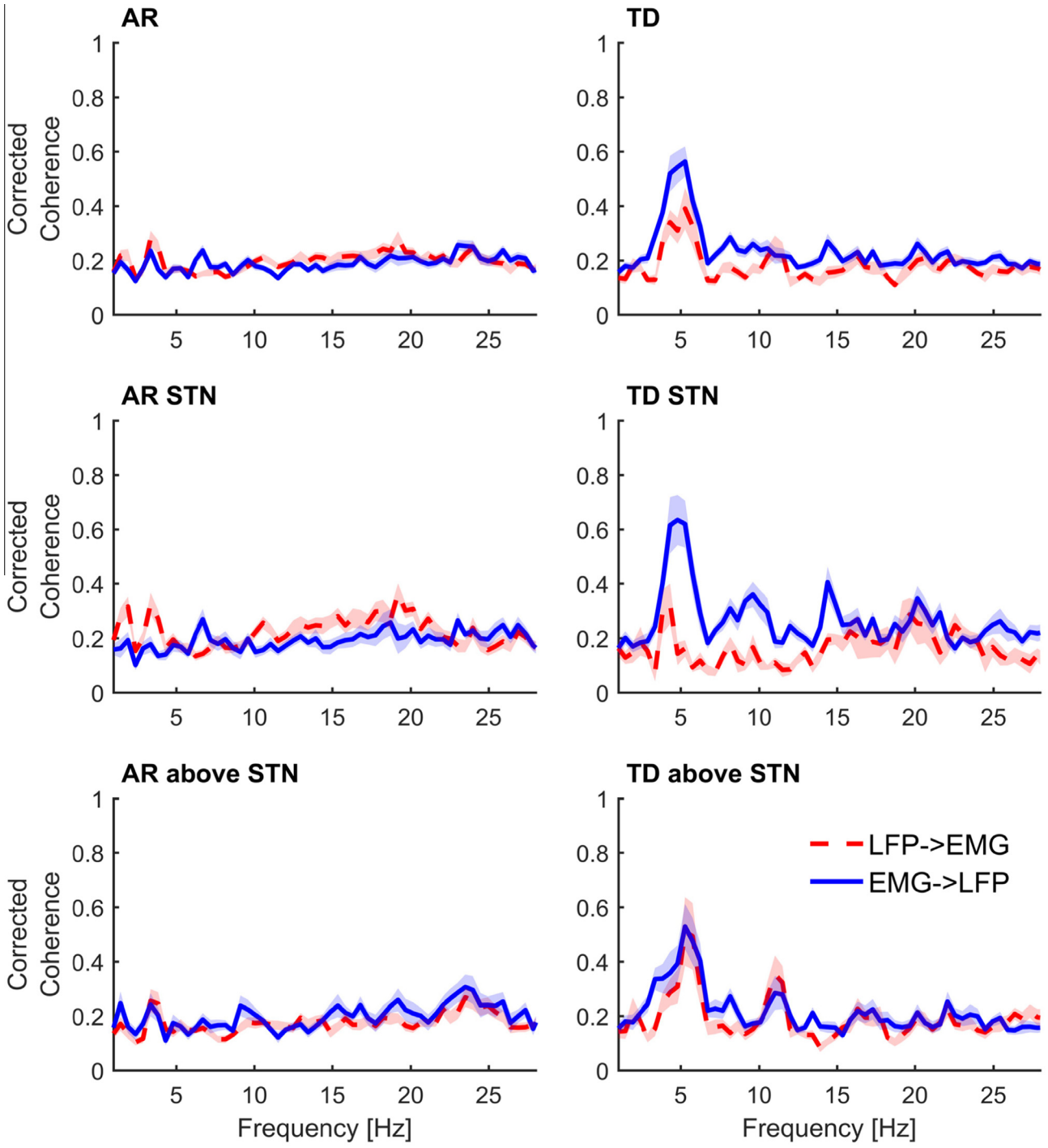

Fig. 4. Average corrected coherence spectra across the significant unidirectional Granger causalities. The shaded areas represent the standard error of the mean. None of the differences are significant after Bonferroni-correction. AR – akinetic-rigid; TD – tremor-dominant; STN – subthalamic nucleus; EMG – electromyogram; LFP – local field potential.

be properly modeled (Schlögl and Supp, 2006). As we are having a rather high sampling rate with 2500 Hz, this means that the frequency resolution with our maximal model order of 50 is not high enough to distinguish 4 Hz steps using Granger causality. We refrained from down-sampling before applying Granger causality, because it potentially destroys the temporal ordering (Florin et al., 2010a). Another alternative could be to use a non-parametric approach of Granger causality (Dhamala et al., 2008). This approach has not yet been tested for its frequency resolution.

Akinetic-rigid and tremor-dominant Parkinson patients

For the TD patients the findings are in accordance with our hypotheses that the afferent connections co-occur with coherence in the tremor- and double tremor-

Table 3. Number of significant unidirectional Granger causalities for the tremor-dominant patients, once with tremor (Tremor) and once without tremor (Iso)

	LFP- > EMG	EMG- > LFP	Total	% LFP- > EMG	% EMG- > LFP	Range LFP- > EMG	Range EMG- > LFP
Iso	13	5	267	4.9	1.9	[0; 11]	[0; 4]
Tremor	20	59	401	5.0	14.7	[0; 9]	[0; 17]
Iso within STN	5	0	91	5.5	0	[0; 5]	[0; 0]
Tremor within STN	1	27	131	0.8	20.6	[0; 1]	[0; 12]
Iso above STN	5	3	109	4.6	2.8	[0; 5]	[0; 3]
Tremor above STN	14	26	217	6.5	12.0	[0; 8]	[0; 12]

Notes: see Table 2.

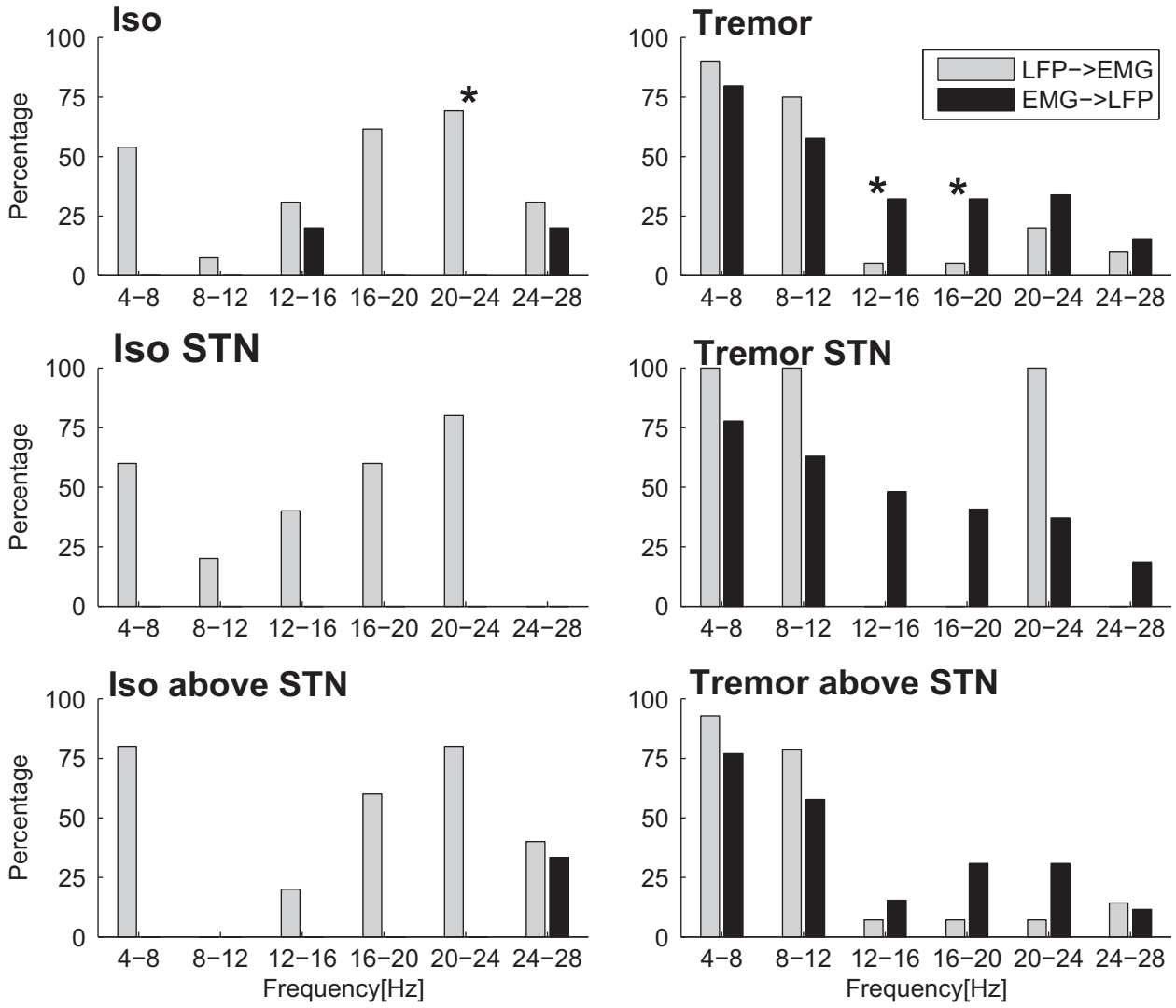

Fig. 5. Co-occurrence of significant causality and coherence during postural-tremor and isometric contraction for the tremor-dominant patients. The graphs display the percentage of connections with a significant coherence in the respective frequency band between EMG and LFP, conditional on the existence of significant unidirectional causal interactions. Across all recording heights during tremor significantly more afferent connections co-occurred with a coherence from 12 to 20 Hz. Tremor – Periods of postural tremor; Iso – Isometric contraction without tremor; STN – subthalamic nucleus; EMG – electromyogram; LFP-local field potential; * – $p \leqslant 0.05$ (see text for exact values).

frequency band. When considering tremor and non-tremor episodes across all recording heights, the same number of efferent and afferent connections was associated with coherence in tremor and double tremor frequency. Interestingly a similar pattern is found when only considering the tremor-episodes, but not the isometric contraction episodes. One has to note for the non-tremor periods of the TD patients that only very few connections were detected. During tremor the almost equal occurrence of efferent and afferent connections in the tremor-frequency range indicates that on the one hand the oscillatory activity from the STN is driving the

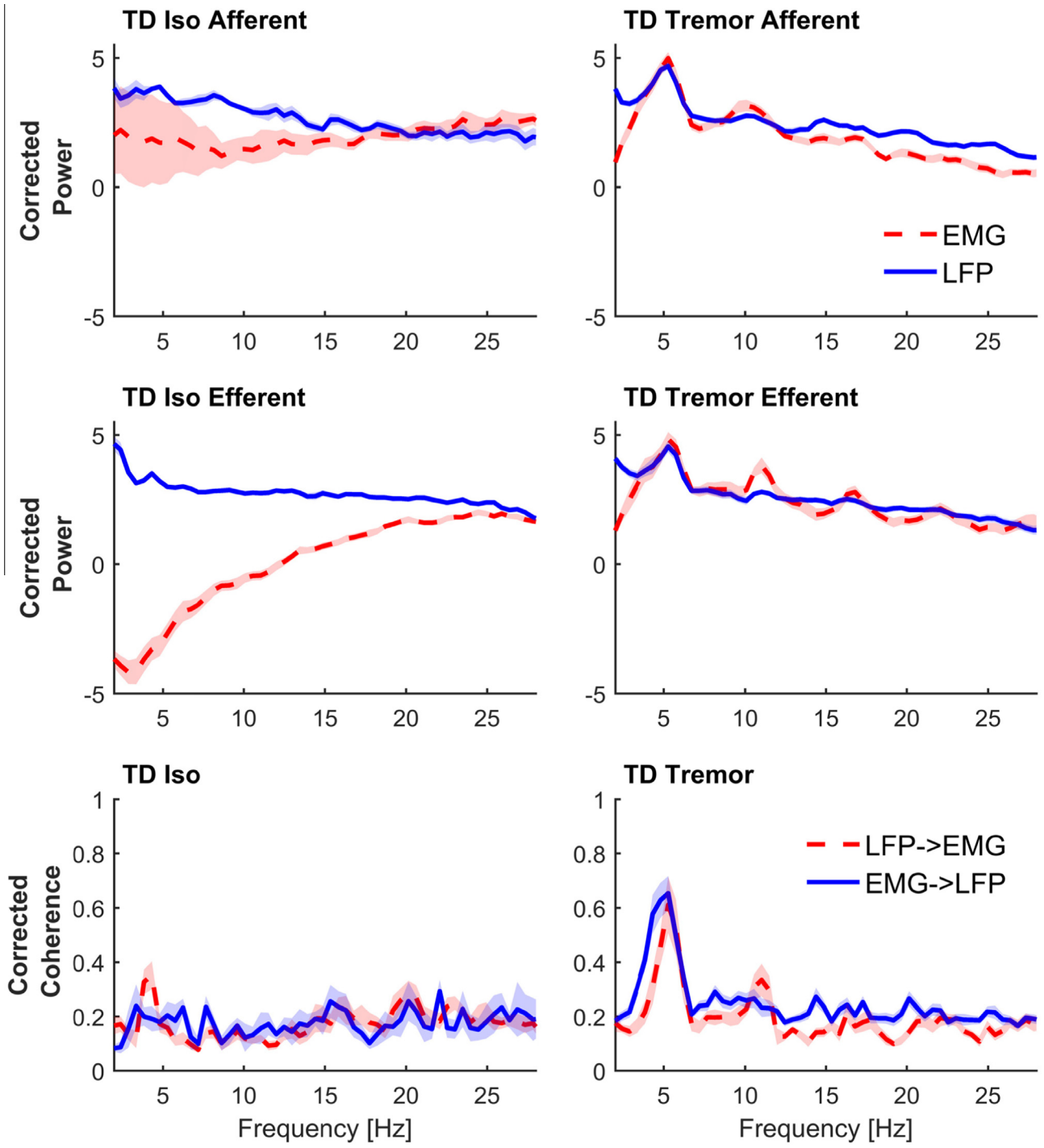

Fig. 6. Average corrected power and coherence spectra across significant unidirectional Granger causalities for the TD patients with and without tremor. The shaded areas represent the standard error of the mean. TD – tremor-dominant; EMG – electromyogram; LFP – local field potential; Iso – isometric contraction; tremor – periods of postural tremor.

tremor and on the other hand that there is a feedback loop. For the AR patients we could not identify a relation between a particular frequency range and the occurrence of causality within the STN. However, for the regions above the STN coherence in the beta frequency range co-occurred with afferent causalities. These findings support the idea that beta oscillations are a pathological hallmark in AR Parkinson patients (Kühn et al., 2006; Weinberger et al., 2006; Brown, 2007). According to the previous literature, beta power increases for AR patients as soon as one enters the STN (Kühn et al., 2005; Chen et al., 2006). Superficially, our results seem to contradict those findings, because we found the co-occurrence of beta coherence and causal connections to be most prominent above the STN. But the present study conditioned the analysis of coherence on the

presence of significant uni-directional causal connections between LFP and EMG, whereas previous findings were unconditional analyses.

As the patients in the current study were performing an isometric contraction, one would expect a reduction in beta oscillatory activity and no coherence in the beta-frequency range (Kühn et al., 2006). Therefore, the significant coherence in the beta-frequency between the contralateral arm EMG and the LFP above the STN for the AR patients is most likely a pathological coupling, which additionally displays an afferent connection.

Coherence as a biomarker for deep brain stimulation?

There is an ongoing search for biomarkers that could potentially be used for improving DBS. In particular, biomarkers predicting the occurrence of a symptom are desired. Both coherence and power can be calculated within a few milliseconds (Florin et al., 2014), making them in principle suitable candidates. Our results, obtained during an isometric hold condition, however, are not encouraging.

For the TD patients during tremor the *tremor-frequency coherence* is accompanied by both afferent and efferent directionality. This indicates that the tremor-signal in the affected arm-muscle and the tremor-activity measured in the STN influence each other. Therefore, before using the tremor-signal within the STN, further studies are needed to identify the relevant signal patterns within the LFP that might predict tremor onset. If such a pattern can be detected, coherence and the activity within the STN might be a potential biomarker. In the case of the AR patients the beta coherence above the STN was associated with significantly more afferent causality, making it an unsuitable candidate for closed-loop stimulation.

As our results have been obtained during an isometric hold condition, future research should investigate whether more promising results can be obtained during rest. In addition, the temporal emergence of coherence as well as power still needs to be investigated in detail. For studying their temporal evolution one would ideally need data where tremor and rigidity develop and vanish. In the present study we only had continuous recordings of hold, preventing us from identifying periods of high and low rigidity/tremor. To further investigate this issue, new carefully planned experiments provoking rigidity/tremor are needed.

CONCLUSION

Our findings of a differential coupling frequency and causality pattern between the two Parkinson subtypes support the idea that different pathways are pathologically altered for the Parkinson subtypes. This knowledge is important to improve the treatment options in a more subtype-targeted approach. The combination of coherence and causality measures in the present study was thus useful to gain further insight into the pathophysiology of PD.

COMPETING INTERESTS

Esther Florin: Grants from the DFG, Montreal Neurological Institute, and Volkswagen Foundation.

Johannes Pfeifer: no conflict of interest.

Veerle Visser-Vandewalle: VVV received payments as a consultant for Medtronic Inc, Boston Scientific, SAPIENS, St. Jude Medical. VVV received honoraria as a speaker on symposia sponsored by Medtronic and St. Jude. Neither VVV nor any member of her family holds stocks, stock options, patents or financial interests in any of the above mentioned companies or their competitors.

Alfons Schnitzler: Grants from the DFG, German Ministry of Education and Research, Helmholtz Society, and Volkswagen Foundation. He served – unrelated to the current project—on scientific advisory boards of Pitie Salpetriere, Novartis, UCB, and Cephalon. He served – unrelated to the current project – as consultant for Medtronic Inc, Boston Scientific, and St. Jude Medical and has received – unrelated to the current project – lecture fees from Boston Scientific, St. Jude Medical, Medtronic GmbH, UCB, MEDA Pharma, Teva Pharma, Boehringer Ingelheim, Novartis, and GlaxoSmithKline.

Lars Timmermann: Lars Timmermann received payments as a consultant for Medtronic Inc, Boston Scientific, SAPIENS, St. Jude Medical, GE Medical, Bayer Healthcare, UCB Schwarz Pharma, Archimedes Pharma. L.T. received honoraria as a speaker on symposia sponsored by TEVA Pharma, Lundbeck Pharma, Bracco, Gianni PR, Medas Pharma, UCB Schwarz Pharma, Desitin Pharma, Boehringer Ingelheim, GlaxoSmithKline, Eumecom, Orion Pharma, Medtronic, Boston Scientific, Cephalon, Abott, GE Medical, Archimedes, and Bayer. The institution of L.T., not L.T. personally received funding by the German Research Foundation, the German Ministry of Education and Research, Manfred und Ursula Müller Stiftung, Klüh Stiftung, Hoffnungsbaum e. V., NBIA Disorders Society USA, Köln Fortune, Medtronic, Deutsche Parkinson Vereinigung, Archimedes Pharma, Abott, Bayer, UCB, zur Rose Pharma, and TEVA. Neither L.T. nor any member of his family holds stocks, stock options, patents or financial interests in any of the above mentioned companies or their competitors.

Acknowledgments—Lars Timmermann announces that this work is supported by the Deutsche Forschungsgemeinschaft (KFO 219; TI 319/2-2) as well as the IMPACT EU-grant (FP7). EF also gratefully acknowledges the support from the DFG (KFO 219; TI 319/2-2).

REFERENCES

Astolfi L, Cincotti F, Mattia D, Marciani MG, Baccala LA, de Vico Fallani F, Salinari S, Ursino M, Zavaglia M, Babiloni F (2006) Assessing cortical functional connectivity by partial directed coherence: simulations and application to real data. IEEE Trans Biomed Eng 53:1802–1812.

Bokil H, Purpura K, Schoffelen JM, Thomson D, Mitra P (2007) Comparing spectra and coherences for groups of unequal size. J Neurosci Methods 159:337–345.

Brown P (2007) Abnormal oscillatory synchronisation in the motor system leads to impaired movement. Curr Opin Neurobiol 17:656–664.

Brown P, Marsden J, Defebvre L, Cassim F, Mazzone P, Oliviero A, Altibrandi MG, Di Lazzaro V, Limousin-Dowsey P, Fraix V, Odin P, Pollak P (2001) Intermuscular coherence in Parkinson's disease: relationship to bradykinesia. NeuroReport 12:2577–2581.

Chen CC, Pogosyan A, Zrinzo LU, Tisch S, Limousin P, Ashkan K, Yousry T, Hariz MI, Brown P (2006) Intra-operative recordings of local field potentials can help localize the subthalamic nucleus in Parkinson's disease surgery. Exp Neurol 198:214–221.

Chen CC, Litvak V, Gilbertson T, Kühn AA, Lu CS, Lee ST, Tsai CH, Tisch S, Limousin P, Hariz M, Brown P (2007) Excessive synchronization of basal ganglia neurons at 20 Hz slows movement in Parkinson's disease. Exp Neurol 205:214–221.

Dhamala M, Rangarajan G, Ding M (2008) Analyzing information flow in brain networks with nonparametric Granger causality. NeuroImage 41:354–362.

Efron B (1981) Nonparametric estimates of standard error: the jackknife, the bootstrap and other methods. Biometrika 68:589–599.

Florin E, Gross J, Pfeifer J, Fink GR, Timmermann L (2010a) The effect of filtering on Granger causality based multivariate causality measures. NeuroImage 50:577–588.

Florin E, Gross J, Reck C, Maarouf M, Schnitzler A, Sturm V, Fink GR, Timmermann L (2010b) Causality between local field potentials of the subthalamic nucleus and electromyograms of forearm muscles in Parkinson's disease. Eur J Neurosci 31:491–498.

Florin E, Gross J, Pfeifer J, Fink GR, Timmermann L (2011) Reliability of multivariate causality measures for neural data. J Neurosci Methods 198:344–358.

Florin E, Himmel M, Reck C, Maarouf M, Schnitzler A, Sturm V, Fink GR, Timmermann L (2012) Subtype-specific statistical causalities in parkinsonian tremor. Neuroscience 210:353–362.

Florin E, Dafsari HS, Reck C, Barbe MT, Pauls KA, Maarouf M, Sturm V, Fink GR, Timmermann L (2013a) Modulation of local field potential power of the subthalamic nucleus during isometric force generation in patients with Parkinson's disease. Neuroscience 240:106–116.

Florin E, Erasmi R, Reck C, Maarouf M, Schnitzler A, Fink GR, Timmermann L (2013b) Does increased gamma activity in patients suffering from Parkinson's disease counteract the movement inhibiting beta activity? Neuroscience 237:42–50.

Florin E, Bock E, Baillet S (2014) Targeted reinforcement of neural oscillatory activity with real-time neuroimaging feedback. NeuroImage 88:54–60.

Gradinaru V, Mogri M, Thompson KR, Henderson JM, Deisseroth K (2009) Optical deconstruction of parkinsonian neural circuitry. Science 324:354–359.

Granger CWJ (1969) Investigating causal relations by econometric models and cross-spectral methods. Econometrica 37:424–438.

Halliday DM, Rosenberg JR, Amjad AM, Breeze P, Conway BA, Farmer SF (1995) A framework for the analysis of mixed time series/point process data–theory and application to the study of physiological tremor, single motor unit discharges and electromyograms. Prog Biophys Mol Biol 64:237–278.

Hilker R, Benecke R, Deuschl G, Fogel W, Kupsch A, Schrader C, Sixel-Doring F, Timmermann L, Volkmann J, Lange M, German Deep Brain Stimulation Association (2009) Deep brain stimulation for Parkinson's disease. Consensus recommendations of the German Deep Brain Stimulation Association. Nervenarzt 80:646–655.

Hirschmann J, Hartmann CJ, Butz M, Hoogenboom N, Ozkurt TE, Elben S, Vesper J, Wojtecki L, Schnitzler A (2013) A direct relationship between oscillatory subthalamic nucleus-cortex coupling and rest tremor in Parkinson's disease. Brain 136:3659–3670.

Kayser AS, Sun FT, D'Esposito M (2009) A comparison of Granger causality and coherency in fMRI-based analysis of the motor system. Hum Brain Mapp 30:3475–3494.

Kühn AA, Williams D, Kupsch A, Limousin P, Hariz M, Schneider GH, Yarrow K, Brown P (2004) Event-related beta desynchronization in human subthalamic nucleus correlates with motor performance. Brain 127:735–746.

Kühn AA, Trottenberg T, Kivi A, Kupsch A, Schneider GH, Brown P (2005) The relationship between local field potential and neuronal discharge in the subthalamic nucleus of patients with Parkinson's disease. Exp Neurol 194:212–220.

Kühn AA, Doyle L, Pogosyan A, Yarrow K, Kupsch A, Schneider GH, Hariz MI, Trottenberg T, Brown P (2006) Modulation of beta oscillations in the subthalamic area during motor imagery in Parkinson's disease. Brain 129:695–706.

Lang AE, Houeto JL, Krack P, Kubu C, Lyons KE, Moro E, Ondo W, Pahwa R, Poewe W, Troster AI, Uitti R, Voon V (2006) Deep brain stimulation: preoperative issues. Mov Disord 21(Suppl. 14): S171–S196.

Reck C, Florin E, Wojtecki L, Groiss S, Voges J, Sturm V, Schnitzler A, Timmermann L (2009a) Differential distribution of coherence between beta-band subthalamic oscillations and forearm muscles in Parkinson's disease during isometric contraction. Clin Neurophysiol 120:1601–1609.

Reck C, Florin E, Wojtecki L, Krause H, Groiss S, Voges J, Maarouf M, Sturm V, Schnitzler A, Timmermann L (2009b) Characterisation of tremor-associated local field potentials in the subthalamic nucleus in Parkinson's disease. Eur J Neurosci 29:599–612.

Reck C, Himmel M, Florin E, Maarouf M, Sturm V, Wojtecki L, Schnitzler A, Fink GR, Timmermann L (2010) Coherence analysis of local field potentials in the subthalamic nucleus: differences in parkinsonian rest and postural tremor. Eur J Neurosci 32:1202–1214.

Schelter B, Winterhalder M, Hellwig B, Guschlbauer B, Lücking CH, Timmer J (2006) Direct or indirect? Graphical models for neural oscillators. J Physiol 99:37–46.

Schlögl A, Supp G (2006) Analyzing event-related EEG data with multivariate autoregressive parameters. In: Neuper, Klimesch, editors. Prog Brain Res, vol. 159. Amsterdam: Elsevier. p. 135–147.

Silberstein P, Kühn AA, Kupsch A, Trottenberg T, Krauss JK, Wohrle JC, Mazzone P, Insola A, Di Lazzaro V, Oliviero A, Aziz T, Brown P (2003) Patterning of globus pallidus local field potentials differs between Parkinson's disease and dystonia. Brain 126:2597–2608.

Spiegel J, Hellwig D, Samnick S, Jost W, Möllers MO, Fassbender K, Kirsch CM, Dillmann U (2007) Striatal FP-CIT uptake differs in the subtypes of early Parkinson's disease. J Neural Transm 114:331–335.

Timmermann L, Gross J, Dirks M, Volkmann J, Freund HJ, Schnitzler A (2003) The cerebral oscillatory network of parkinsonian resting tremor. Brain 126:199–212.

Volkmann J, Joliot M, Mogilner A, Ioannides AA, Lado F, Fazzini E, Ribary U, Llinas R (1996) Central motor loop oscillations in parkinsonian resting tremor revealed by magnetoencephalography. Neurology 46:1359–1370.

Weinberger M, Mahant N, Hutchison WD, Lozano AM, Moro E, Hodaie M, Lang AE, Dostrovsky JO (2006) Beta oscillatory activity in the subthalamic nucleus and its relation to dopaminergic response in Parkinson's disease. J Neurophysiol 96:3248–3256.

Welch PD (1967) The use of fast Fourier transform for the estimation of power spectra: a method based on time averaging over short, modified periodograms. IEEE Trans Audio Electroacoust 15:70–73.

(Accepted 29 June 2016)
(Available online 5 July 2016)